Journal of Catalysis **186,** 75–80 (1999)
Article ID jcat.1999.2534, available online at http://www.idealibrary.com on IDEAL®

Activity Control by Structural Design of Multicomponent Scheelite-Type Molybdate Catalysts for the Selective Oxidation of Propene

Yo-Han Han,* Wataru Ueda,†,[1] and Yoshihiko Moro-Oka*

*Research Laboratories of Resources Utilization and †Department of Environmental Chemistry and Engineering, Tokyo Institute of Technology, 4259, Nagatsuta-cho, Midori-ku, Yokohama 226-0087, Japan

Received December 15, 1998; revised April 14, 1999; accepted April 21, 1999

Control of the catalytic selective oxidation of propene to acrolein was achieved by designing multicomponent metal oxide catalysts to have the multifunctions required for the reaction, such as activation of allylic hydrogen of propene, oxygen insertion, reduction–oxidation coupling, lattice oxygen mobility, and activation of molecular oxygen. Scheelite-type $Na_{0.5-3x}La_{0.5+x}MoO_4$ oxides having lattice oxide ion mobility were chosen as a basic catalytic material and used as a support for bismuth molybdate and cerium oxide loadings. The catalytic activity was primarily controlled by the introduction of lanthanum into the $Na_{0.5-3x}La_{0.5+x}MoO_4$ lattice, and the selectivity to acrolein was attained separately by loading bismuth molybdates on the surface of the support. It was found that the catalytic activity of $Bi_2Mo_3O_{12}/Na_{0.5-3x}La_{0.5+x}MoO_4$ is strongly governed by the value of x irrespective of the loading of $Bi_2Mo_3O_{12}$. It was also demonstrated that high activities exceeding the primary activity were achieved by designedly introducing cerium both into the surface bismuth molybdate phase and in the vicinity of the surface of the scheelite support.

Key Words: **multicomponent bismuth molybdate catalyst; scheelite structure; selective oxidation; propene; acrolein.**

1. INTRODUCTION

Gas-phase oxidation and ammoxidation of lower olefins to produce the corresponding unsaturated aldehydes and nitriles have been widely industrialized by using complicated multicomponent metal oxide catalyst systems mostly including bismuth molybdate as a key catalyst component (1–4). It is generally accepted that bismuth molybdate is located on the surface of the catalyst particle and works as a main active site in these catalyst systems. On the other hand, transition metal molybdates are concentrated in the bulk of the particle and act not only as a support for the active components but also as an oxygen reservoir (5–9).

In contrast to the above multicomponent and multiphasic metal oxide catalysts consisting of bismuth molybdates, multicomponent bismuth molybdate catalysts having the scheelite (ABO_4) structure, where metal cations other than molybdenum, such as bismuth usually have ionic radii larger than 0.9 Å, are monophasic. In the scheelite structure (ABO_4-type), the A cation is usually divalent and eight-coordinated by oxygen while the B cation is hexavalent and appears as discrete BO_4 tetrahedra in the structure. When molybdates of monovalent and trivalent metal cations crystallize into a scheelite structure with general formula $A^{+1}_{0.5-3x}A^{3+}_{0.5+x}\phi_{2x}MoO_4$, one trivalent cation is replaced by three monovalent cations and two cation vacancies (ϕ) are formed.

These lattice vacancies in the structure are very important in scheelite-type catalysts (10–17). The suggested role of the cation vacancy is to stabilize protons formed in the rate-determining dissociative adsorption of propene onto a π-allyl intermediate (10). However, Grasselli *et al.* have concluded from their mechanistic studies that initial chemisorption occurs on coordinatively unsaturated molybdenum centers, while allylic hydrogen abstraction takes place on oxygen bonded to bismuth, but cation vacancies generate molybdenyl-type functionalities which are responsible for the insertion of oxygen into the allylic intermediate (14, 20). The increase in cation vacancies in the system also accelerates the bulk migration of the lattice oxide ion which is involved exclusively in the catalytic reaction. The importance of high mobility of oxide ions was demonstrated in the $Bi_{1-3x}V_{1-x}Mo_xO_4$ system using an ^{18}O tracer (18, 19). In other words, it is possible to control oxidation activity of oxide catalysts by controlling lattice oxygen mobility in the bulk under catalytic oxidation conditions.

In the present study, we have tried to control propene oxidation activity and selectivity of complex oxide catalysts by designing multifunctions required for the reaction, such as activation of allylic hydrogen of propene, oxygen insertion, reduction–oxidation coupling, lattice oxygen mobility, and activation of molecular oxygen, as proposed by the Grasselli school (15, 21, 22) and based on our water-tank concept (1). For this purpose we chose $Na_{0.5-3x}La_{0.5+x}MoO_4$, which has a scheelite structure in which the lattice

[1] To whom correspondence should be addressed at Department of Materials Science and Engineering, Science University of Tokyo in Yamaguchi, Daigaku-dori, 1-1-1, Onoda-shi, Yamaguchi 756-0884 Japan.

0021-9517/99 $30.00

oxygen mobility and the activation of molecular oxygen can be controlled by changing the content of the lattice vacancies. To add functions indispensable for yielding acrolein selectively, such as allylic hydrogen abstraction and oxygen insertion, the scheelite oxides are covered with bismuth molybdates. Finally Ce^{3+} is introduced onto the surface of the scheelite base oxides to achieve effective reduction–oxidation (15, 21, 22).

2. METHODS

2.1. Catalyst Preparation

Sodium lanthanomolybdate scheelite oxides ($Na_{0.5-3x}La_{0.5+x}MoO_4$) were prepared by coprecipitation. An aqueous solution containing the stoichiometrically desired amount of $(NH_4)_6Mo_7O_{24}\cdot 4H_2O$ was slowly added dropwise at room temperature to an aqueous solution containing the desired amounts of $NaNO_3$ and $La(NO_3)_3\cdot 6H_2O$. The pH of the solution was adjusted to 7 by the addition of 28% ammonia solution. The suspension was stirred at 80°C until evaporation was almost complete. The product was then dried at 120°C for 10 h, ground, and heated to 300°C for 5 h to decompose the nitrates. The heated powder was then reground and finally heated in air at 650°C for 4 h.

Sodium lanthanomolybdate-supported bismuth molybdate catalysts were prepared according to the method reported by He *et al.* (5). Sodium lanthanomolybdate was first impregnated with ammonium molybdate solution. After being dried by evaporation, it was again impregnated with an ethanol solution of triphenylbismuth and evaporated until dry. The resulting mass was further dried at 130°C for 3 h, ground, and calcined in air at 450°C for 2 h. Cerium oxide was also supported in various impregnation orders by the same impregnation method with $Ce(NO_3)_3\cdot 6H_2O$ aqueous solution. The bismuth molybdate and cerium oxide were supported on sodium lanthanomolybdate in various loading amounts; e.g., the molar ratio of $Bi_2Mo_3O_{12}$ and Ce_2O_3 in $Bi_2Mo_3O_{12}$ (or Ce_2O_3)/$Na_{0.5-3x}La_{0.5+x}\phi_{2x}MoO_4$ was from 0 to 0.005. The atomic ratio Bi/Mo was always 2/3. The catalysts were characterized by XRD, BET, and XPS measurements. The powder X-ray diffraction patterns were recorded with steps of 0.02° over the angle range 10–85° at 0.5°/min using an X-ray diffractometer with Cu$K\alpha$ radiation. Cell dimensions were obtained by least-squares treatment of the data. Surface area was measured by nitrogen adsorption using the BET method. The XPS measurements were performed with the $Bi_2Mo_3O_{12}$ and Ce_2O_3 catalysts supported on $Na_{0.5-3x}La_{0.5+x}MoO_4$ for C_{1s}, O_{1s}, Na_{1s}, Mo_{3d}, La_{3d}, Ce_{3d}, and Bi_{4f}. The Bi/*Me*, Ce/*Me*, Na + La/*Me*, Mo/*Me* (*Me* = Bi + Ce + Na + La + Mo), and Bi/Ce ratios were calculated from XPS intensities using the atomic sensitivity factors provided. Bulk ratios of the above metals were calculated from the sample stoichiometry in the preparation.

2.2. Reaction Procedure

Catalytic activities of bismuth molybdate and cerium oxide supported on sodium lanthanomolybdates for the oxidation of propene to acrolein were examined using a conventional pulse reactor. The reactant gas mixture (propene/O_2 = 1/2, 0.6 ml STP) was injected into the reactor using a gas syringe. The helium flow through the column was held at 10 $cm^3\,min^{-1}$ at a head pressure of 40 p.s.i.g. The reaction temperature was kept at 400°C and the catalyst weight was 0.40 g constant. The reaction products were analyzed using a gas chromatograph equipped with both flame-ionization and thermal-conductivity detectors.

3. RESULTS AND DISCUSSION

3.1. Activity and Selectivity Control in $Na_{0.5-3x}La_{0.5+x}MoO_4$-Supported $Bi_2Mo_3O_{12}$ Catalysts

One of the most fruitful approaches for developing new or better solid-state catalysts is to identify the required catalytic functions and then to incorporate them into the catalyst. An understanding of catalytic chemistry of fundamental catalytic functions is obviously very important. In catalytic selective oxidations, the following fundamental catalytic functions would be listed: (1) acid–base function for controlling adsorption and desorption of organic molecules and for activating adsorbed species in desired ways, (2) coordinatively unsaturated surface entrances generated by particular surface structure for providing a field for bond formation and arrangement of adsorbed species, (3) redox functions for controlling oxidation state of catalyst elements and for activating molecular oxygen, and (4) synergy effects achieved by electron transfer and surface or bulk transfer of reaction elements during catalysis. In the present study for designing multifunctional catalysts for propene selective oxidation to acrolein, the $Bi_2Mo_3O_{12}$ phase was selected for construction of functions (1) and (2), cerium oxide for function (3), and scheelite-type sodium lanthanomolybdate, $Na_{0.5-3x}La_{0.5+x}MoO_4$ for function (4). The combination of functions (1), (2), and (4) was studied first. We employed a supported catalyst system for better control of each function.

First we characterized the supported catalysts to determine if the catalysts had the desired structures of the catalyst design. Summarized in Table 1 are the cell parameters of the scheelite phase $Na_{0.5-3x}La_{0.5+x}MoO_4$ system and the $Na_{0.5-3x}La_{0.5+x}MoO_4$-supported $Bi_2Mo_3O_{12}$ system ($Bi_2Mo_3O_{12}$/$Na_{0.5-3x}La_{0.5+x}MoO_4$), the BET surface areas, and the propene conversion and selectivity to acrolein. All observed diffractions in the X-ray powder patterns of $Na_{0.5-3x}La_{0.5+x}MoO_4$ were unambiguously assigned to the tetragonal scheelite structure (space group $I41/a$) which persisted over the range of x from 0 to 0.08.

TABLE 1

Characterization Data and Catalytic Performance of $Na_{0.5-3x}La_{0.5+x}MoO_4$ and $Bi_2Mo_3O_{12}/Na_{0.5-3x}La_{0.5+x}MoO_4$

Catalyst	x	Lattice parameter a (Å)	Lattice parameter c (Å)	BET surface area (m^2/g)	Propene conversion (%)	Acrolein selectivity (%)
$Na_{0.5-3x}La_{0.5+x}MoO_4$	0	5.343	11.730	0.6	0.8	48.5
	0.03	5.346	11.760	1.1	10.2	45.5
	0.08	5.353	11.814	1.3	15.3	37.7
$Bi_2Mo_3O_{12}/Na_{0.5-3x}La_{0.5+x}MoO_4$(0.0025)	0	5.341	11.727	0.7	1.2	64.9
	0.03	5.346	11.764	0.7	13.0	61.7
	0.08	5.354	11.797	0.7	22.2	77.1

Note. Catalyst, 0.4 g; 400°C; pulse: propene/oxygen = 1/2, 0.6 ml, data after 10 pulses.

The lattice parameters changed linearly with x, indicating random replacement of sodium cations by lanthanum in the structure with the formation of lattice structural defects. The result certifies that the function (4) is introduced into the support having the scheelite structure, since it is known that the defects assist the migration of lattice oxide ions.

The supported system, $Bi_2Mo_3O_{12}/Na_{0.5-3x}La_{0.5+x}MoO_4$, showed no XRD peaks ascribed to bismuth oxide, molybdenum oxide, or any composite oxide among Mo, Bi, Na, and La, except the pattern of the scheelite phase. It was found, however, that the loading of $Bi_2Mo_3O_{12}$ did not affect the lattice parameters of the scheelite structure (Table 1). The result reveals that most of the bismuth loaded was located on the surface. There might be a possibility that small amounts of bismuth incorporate into the scheelite lattice, but the effect of the incorporated bismuth on the function (4) would be negligible.

The surface deposition of bismuth is supported by XPS analysis for the elemental composition of each catalyst, as shown in Table 2. The XPS measurement was carried out before and after catalytic reaction. The ratio of Mo/*Me* (*Me* = Bi + Na + La + Mo) on the surface of every catalyst was higher than that of the bulk calculated from stoichiometry. In contrast the Na + La/*Me* ratios were lower than those of the bulk and high in the supported catalysts. The Bi/*Me* ratios of the supported catalysts were 10–20 times larger than those from the calculated bulk compositions. These results clearly show that the loaded bismuth predominantly locates on the surface of the $Na_{0.5-3x}La_{0.5+x}MoO_4$ catalysts and forms finely dispersed crystals of bismuth molybdate phases by reaction with the surface excess molybdenum and/or the loaded molybdenum, although no XRD peaks corresponding to the bismuth molybdate phases were observed. It can be assumed that the still remaining excess molybdenum on the surface forms free molybdenum oxide clusters. Since the surface element ratios did not change greatly after the catalytic reaction (10 pulses at 400°C), the surface state of the catalysts appears to persist during the catalytic reaction. The above trends were not affected by the content of La or by its use for the catalytic reaction. As a consequence, the construction of surface bismuth molybdates was nicely achieved, suggesting functions (1) and (2).

We tested the catalytic performance of the above-designed catalyst for propene oxidation. The catalytic behavior of $Na_{0.5-3x}La_{0.5+x}MoO_4$ ($x = 0$–0.08) and $0.0025Bi_2Mo_3O_{12}/Na_{0.5-3x}La_{0.5+x}MoO_4$ ($x = 0$–0.08) in selective oxidation of propene at 400°C is shown in Table 1. The catalytic activity of $Na_{0.5-3x}La_{0.5+x}MoO_4$ was dramatically increased by the introduction of La, because the mobility of lattice oxide ions is enhanced by defects formed in the lanthanum-substituted scheelite catalysts. This fact is not controlled by surface area, which as a result is very small and deviates little in each catalyst. On the other hand, the selectivity to acrolein slightly decreased instead of increasing.

TABLE 2

Surface and Bulk Compositions of the Elements in $Bi_2Mo_3O_{12}/Na_{0.5-3x}La_{0.50+x}MoO_4$

Catalyst	Bi/*Me*	Na + La/*Me*	Mo/*Me*
$Na_{0.50}La_{0.50}MoO_4$			
Before reaction	—	0.34	0.66
After reaction	—	0.32	0.68
Bulk	—	(0.50)	(0.50)
$Bi_2Mo_3O_{12}/Na_{0.50}La_{0.50}MoO_4$(0.0025/1)			
Before reaction	0.058	0.27	0.68
After reaction	0.039	0.30	0.66
Bulk	(0.0025)	(0.50)	(0.50)
$Na_{0.41}La_{0.53}MoO_4$			
Before reaction	—	0.33	0.67
After reaction	—	0.35	0.65
Bulk	—	(0.48)	(0.52)
$Bi_2Mo_3O_{12}/Na_{0.41}La_{0.53}MoO_4$(0.0025/1)			
Before reaction	0.029	0.27	0.70
After reaction	0.029	0.29	0.68
Bulk	(0.0025)	(0.48)	(0.52)

Note. *Me* = Bi + Na + La + Mo.

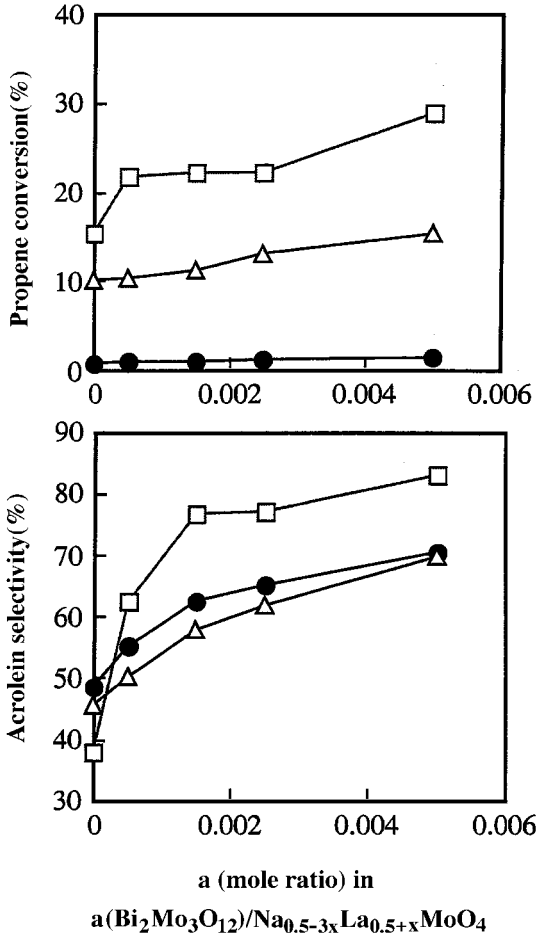

FIG. 1. Effect of $Bi_2Mo_3O_{12}$ loading on $Na_{0.5-3x}La_{0.5+x}MoO_4$ catalysts ($x = 0$ (●), 0.03 (△), and 0.08 (□)) for propene oxidation to acrolein.

In the case of the supported catalysts, it can be seen that the loading of $Bi_2Mo_3O_{12}$ to $Na_{0.5-3x}La_{0.5+x}MoO_4$ has a small enhancement effect on the catalytic activity. Practically the same conversions were attained when the lanthanum content (x) was the same in both the nonsupported and the supported catalysts, indicating that the activity is mainly governed by function (4) of the support, not by the supported bismuth molybdates. In contrast to the activity, the selectivity to acrolein was appreciably improved by the loading. This can be seen more clearly in Fig. 1, where the propene conversion and selectivity to acrolein over the $Bi_2Mo_3O_{12}/Na_{0.5-3x}La_{0.5+x}MoO_4$ catalysts are shown as functions of x and the $Bi_2Mo_3O_{12}$ loading amount. The figure demonstrates again that the catalytic activity of $Bi_2Mo_3O_{12}/Na_{0.5-3x}La_{0.5+x}MoO_4$ is strongly governed by the value of x irrespective of the $Bi_2Mo_3O_{12}$ loading amount. More importantly the figure shows clear increases in acrolein selectivity with the increase in the loading amount. Obviously, functions (1) and (2) of the supported bismuth molybdates are working to generate of acrolein selectivity.

3.2. *Redox Control by Ce_2O_3 in $Na_{0.5-3x}La_{0.5+x}MoO_4$-Supported $Bi_2Mo_3O_{12}$ Catalysts*

The above results on the designed catalysts clearly demonstrated that the catalytic activity of the surface bismuth molybdates having functions (1) and (2) is apparently controlled by function (4) of the support. However, one should not assume that function (4), in other words, the migration rate of lattice oxide ions, determines the oxidation rate, since the rate-determining step is hydrogen abstraction from adsorbed propene. The principal functions (1) and (2) of the surface bismuth molybdate determine the rate of oxidation into the desired products and are sustained by function (4) of the support. If function (3), the redox function, effectively operates between functions (1) and (2) and function (4), the statistical number of active sites having the former functions will increase, resulting in an increase in activity. In fact, one might see appreciable increases in propene conversion with increased loading of bismuth in Fig. 1 and this small change is considered to result from the fact that excess bismuth plays the role of function (3) on the surface. We, therefore, investigated the effect of Ce_2O_3 addition instead of bismuth addition on the catalytic properties of the $Bi_2Mo_3O_{12}/Na_{0.5-3x}La_{0.5+x}MoO_4$ catalyst system.

The effect of Ce_2O_3 addition to $Bi_2Mo_3O_{12}/Na_{0.5-3x}La_{0.5+x}MoO_4$ on the catalytic performance in the selective oxidation of propene to acrolein is shown in Fig. 2. As

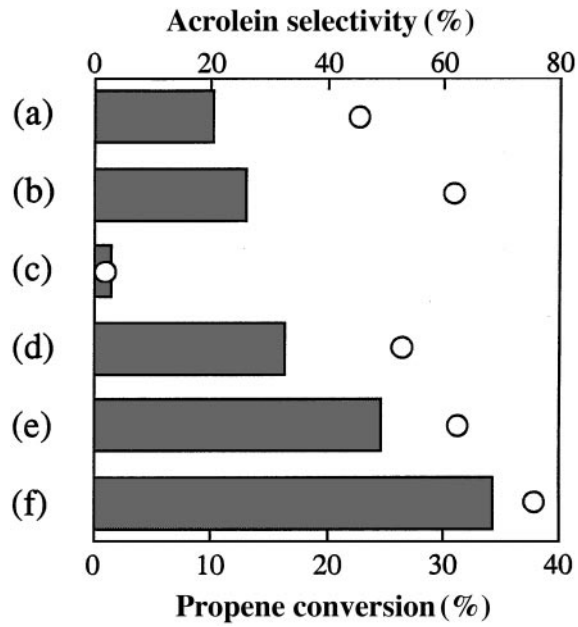

FIG. 2. Propene conversion (■) and selectivity to acrolein (○) in propene oxidation over (a) $Na_{0.41}La_{0.53}MoO_4$, (b) $Bi_2Mo_3O_{12}/Na_{0.41}La_{0.53}MoO_4$(0.0025/1), (c) $Ce_2O_3/Na_{0.41}La_{0.53}MoO_4$(0.0025/1), (d) $Ce_2O_3/Bi_2Mo_3O_{12}/Na_{0.41}La_{0.53}MoO_4$(0.0025/0.0025/1), (e) Ce_2O_3–$Bi_2Mo_3O_{12}/Na_{0.41}La_{0.53}MoO_4$(0.0025–0.0025/1), and (f) $Bi_2Mo_3O_{12}/Ce_2O_3/Na_{0.41}La_{0.53}MoO_4$(0.0025/0.0025/1).

described above, the simple loading of $Bi_2Mo_3O_{12}$ onto the $Na_{0.41}La_{0.53}MoO_4$ support did not result in a drastic increase in catalytic activity. The loading of Ce_2O_3 alone did not increase the activity but rather suppressed the activity and the selectivity. We then tested the loading of both, which is modified by varying the supporting order of Ce_2O_3 and $Bi_2Mo_3O_{12}$ on $Na_{0.41}La_{0.53}MoO_4$. As shown in Fig. 2, the catalytic activity and selectivity to acrolein increased in the following order: $Ce_2O_3/Bi_2Mo_3O_{12}/Na_{0.41}La_{0.53}MoO_4$ < $Bi_2Mo_3O_{12}$-$Ce_2O_3/Na_{0.41}La_{0.53}MoO_4$ < $Bi_2Mo_3O_{12}/Ce_2O_3/Na_{0.41}La_{0.53}MoO_4$. The catalyst that was prepared by loading first Ce_2O_3 onto the support and then $Bi_2Mo_3O_{12}$ showed the highest activity and selectivity. The second catalyst was prepared by loading cerium and bismuth simultaneously. The third was prepared by loading Ce_2O_3 after supporting bismuth. The effect of Ce_2O_3 loading on activity is very clear in every Ce_2O_3-loaded catalyst. The most prominent effect appears in the $Bi_2Mo_3O_{12}/Ce_2O_3/Na_{0.41}La_{0.53}MoO_4$ catalyst, which has activity three times higher than that of the pure $Na_{0.41}La_{0.53}MoO_4$ catalyst and is fairly selective for the formation of acrolein.

The promotion effect of cerium on the $Bi_2Mo_3O_{12}/Na_{0.5-3x}La_{0.5+x}MoO_4$ catalyst is more clearly demonstrated in Fig. 3, where catalytic activity and selectivity to acrolein of catalysts loading bismuth molybdates in different amounts are shown as a function of the extent of lanthanum substitution (x). In the case of the cerium-free supported catalysts, it was seen that the activity is mainly governed by function (4) of the support. Exactly the same thing happened in the cerium-loaded supported catalysts, as can be seen in Fig. 3. Therefore, whether the catalysts contain cerium or not, the catalyst on the support having no function (4) never shows good activity for propene oxidation. Once the support gains function (4), high activities are achieved and more activities are achieved by the introduction of function (3) from cerium. The selectivity to acrolein was almost independent of the presence of cerium, suggesting that the selectivity is mainly governed by functions (1) and (2) from the surface bismuth molybdate phase. Here again, functions (1) and (2) of the supported bismuth molybdates are working.

Before concluding that function (3) is effective, we characterized the bulk state by XRD and the surface composition by XPS as was done for the Ce_2O_3-free catalysts. Neither $Bi_2Mo_3O_{12}$ nor any composite oxides among Ce, Bi, Na, La, and Mo were detected in the cerium-containing catalysts except in the scheelite phase. In addition, no appreciable lattice parameter changes were observed. Accordingly, we consider that cerium is finely dispersed on the surface of $Na_{0.41}La_{0.53}MoO_4$ irrespective of the supporting procedure.

The XPS data for each catalyst are shown in Table 3. It was observed that the Na + La/*Me* (*Me* = Bi + Ce + Na + La + Mo) ratios were lower than those from the calcu-

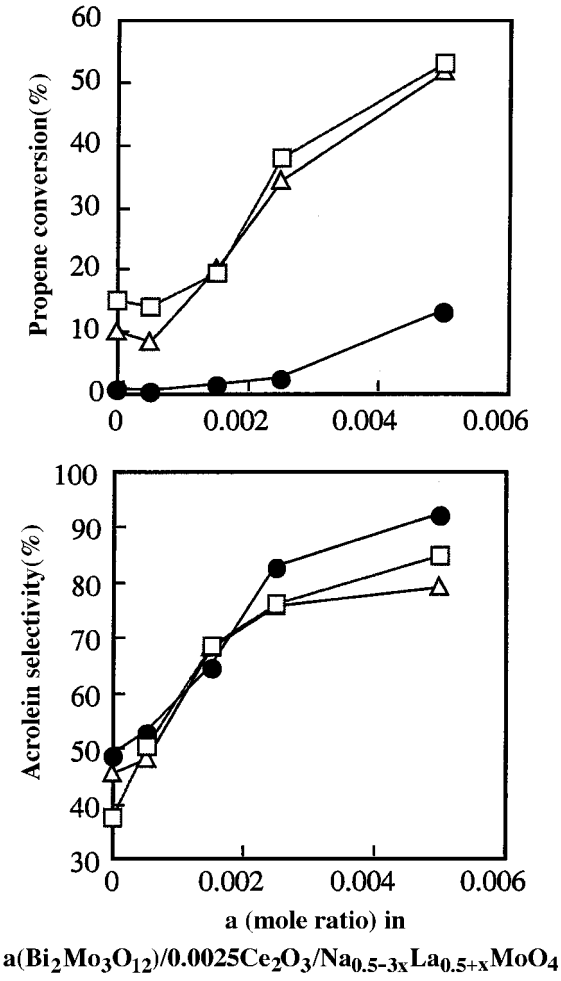

FIG. 3. Effect of $Bi_2Mo_3O_{12}$ loading on $Ce_2O_3/Na_{0.5-3x}La_{0.5+x}MoO_4$ (0.0025/1) catalysts ($x = 0$ (●), 0.03 (△), 0.08 (□)) for propene oxidation to acrolein.

lated bulk compositions, and the Bi/*Me* and Ce/*Me* ratios of the Ce_2O_3/ and $Bi_2Mo_3O_{12}/Na_{0.5-3x}La_{0.5+x}MoO_4$ catalysts were higher, indicating that the Ce and Bi are concentrated on the surface of the $Na_{0.5-3x}La_{0.5+x}MoO_4$ support, as naturally expected from the supporting procedure. According to the supporting order of Ce_2O_3 and $Bi_2Mo_3O_{12}$, the Bi/*Me*, Bi/Ce, and Ce/*Me* ratios changed regularly: (1) the catalyst in which $Bi_2Mo_3O_{12}$ is supported first and then Ce_2O_3 shows the highest Ce/*Me* ratio and the lowest Bi/*Me* and Bi/Ce ratios among the three catalysts, (2) the catalyst in which $Bi_2Mo_3O_{12}$ and Ce_2O_3 were simultaneously supported shows moderate Ce/*Me*, Bi/*Me*, and Bi/Ce ratios, and (3) the catalyst in which Ce_2O_3 is supported first and then $Bi_2Mo_3O_{12}$ shows the lowest Ce/*Me* ratio and the highest Bi/*Me* and Bi/*Me* ratios. The results definitely support the conclusion that the surface structure of the supported catalysts is determined by the supporting procedure. It was ascertained that the surface area was not varied by the loading of Ce_2O_3 and was not affected by the

TABLE 3

Surface and Bulk Composition of the Elements in Ce_2O_3 and $Bi_2Mo_3O_{12}$ Catalysts Supported on $Na_{0.5-3x}La_{0.50+x}MoO_4$

Catalyst	Bi/*Me*	Ce/*Me*	Na + La/*Me*	Mo/*Me*	Bi/Ce
$Ce_2O_3/Bi_2Mo_3O_{12}/Na_{0.41}La_{0.53}MoO_4$(0.0025/0.0025/1)					
Before reaction	0.040	0.056	0.24	0.66	0.71
After reaction	0.035	0.046	0.21	0.71	0.76
Bulk	(0.0025)	(0.0025)	(0.48)	(0.52)	(1.0)
Ce_2O_3–$Bi_2Mo_3O_{12}/Na_{0.41}La_{0.53}MoO_4$(0.0025–0.0025/1)					
Before reaction	0.069	0.042	0.23	0.66	1.6
After reaction	0.058	0.026	0.27	0.64	2.2
Bulk	(0.0025)	(0.0025)	(0.48)	(0.52)	(1.0)
$Bi_2Mo_3O_{12}/Ce_2O_3/Na_{0.41}La_{0.53}MoO_4$(0.0025/0.0025/1)					
Before reaction	0.077	0.016	0.24	0.66	4.8
After reaction	0.059	0.023	0.25	0.67	2.6
Bulk	(0.0025)	(0.0025)	(0.48)	(0.52)	(1.0)

Note. $Me = Bi + Ce + Na + La + Mo$.

catalytic reaction. The Ce/*Me*, Bi/*Me*, and Bi/Ce ratios were not drastically changed either after the reaction.

On the basis of the above structural and surface characterization, we can now conclude that function (3), the redox function, provided by cerium in the present designed catalysts is very important for achieving high activity and selectivity, and probably for catalyst stability as well. As function (3), the redox couple Ce^{3+}/Ce^{4+} assists oxygen and electron transfer in every phase in the supported catalysts and also promotes dioxygen reduction. However, the location of cerium in the catalyst is highly crucial, as demonstrated in Fig. 2. Since the highest activity was attained over the catalyst having the highest Bi/Ce ratio or the lowest surface concentration of cerium (Table 3), cerium should be located between the support and the active bismuth molybdate phase to achieve intercommunication of each function, which turns out to produce high activity. It seems that cerium is located both in the surface bismuth molybdate phase and in the vicinity of the surface of the scheelite support. This situation seems to provide a very efficient redox process.

4. CONCLUSIONS

Catalytic activity and selectivity of scheelite-type multicomponent metal oxide catalysts for oxidation of propene to acrolein was controlled by designing locations of constituents in and on the catalyst particles. Generation of oxidation selectivity was achieved by surface bismuth molybdate supported on scheelite-type $Na_{0.5-3x}La_{0.5+x}MoO_4$ oxides. The catalytic activity was controlled both by the mobility of lattice oxide ions and by the presence of the redox couple Ce^{3+}/Ce^{4+}. The catalytic activity was primarily controlled by the introduction of lanthanum into the $Na_{0.5-3x}La_{0.5+x}MoO_4$ lattice enhancing the mobility of lattice oxide ions. It was also demonstrated that high activities exceeding the primary activity were achieved by intentionally introducing cerium both into the surface bismuth molybdate phase and in the vicinity of the surface of the scheelite support.

REFERENCES

1. Moro-oka, Y., and Ueda, W., *Adv. Catal.* **40**, 233 (1994).
2. Weng, L. T., and Delmon, B., *Appl. Catal. A* **81**, 141 (1991).
3. Keulks, G. W., Krenzke, L. D., and Noterdam, T. M., *Adv. Catal.* **27**, 183 (1978).
4. Bordes, E., *in* "Studies in Surface Science and Catalysis" (R. K. Grasselli and A. W. Sleight, Eds.), Vol. 79, p. 21. Elsevier, Amsterdam, 1991.
5. He, D. H., Ueda, W., and Moro-oka, Y., *Catal. Lett.* **12**, 35 (1992).
6. Brazdil, J. F., Suresh, D. D., and Grasselli, R. K., *J. Catal.* **66**, 347 (1980).
7. Wolfs, M. W. J., and Batist, Ph. A., *J. Catal.* **55**, 25 (1974).
8. Matsuura, I., and Wolfs, M. W. J., *J. Catal.* **37**, 174 (1975).
9. Matsuura, I., *in* "Proceedings, 7th International Congress on Catalysis, Tokyo, 1980" (T. Seiyama and K. Tanabe, Eds.), Part B, p. 1009. Elsevier, Amsterdam, 1981.
10. Sleight, A. W., *in* "Advanced Materials in Catalysis" (J. J. Barton and R. L. Garten, Eds.), p. 181. Academic Press, New York, 1977.
11. Aykan, K., Sleight, A. W., and Rogers, D. B., *J. Catal.* **29**, 185 (1973).
12. Linn, W. J., and Sleight, A. W., *J. Catal.* **41**, 134 (1976).
13. Sleight, A. W., Aykan, K., and Rogers, D. B., *J. Solid State Chem.* **13**, 231 (1975).
14. Brazdil, J. F., Gleaser, L. C., and Grasselli, R. K., *J. Catal.* **81**, 142 (1983).
15. Brazdil, J. F., and Grasselli, R. K., *J. Catal.* **79**, 104 (1983).
16. De Rossi, S., Lo Jacono, M., Porta, P., Valigi, M., Gazzoli, D., Minelli, G., and Anichini, A., *J. Catal.* **100**, 95 (1986).
17. De Rossi, S., Lo Jacono, M., Gardini, M., and Porta, P., *J. Catal.* **146**, 126 (1994).
18. Ueda, W., Asakawa, K., Chen, C.-L., Moro-oka, Y., and Ikawa, T., *J. Catal.* **101**, 360 (1986).
19. Ueda, W., Chen, C.-L., Asakawa, K., Moro-oka, Y., and Ikawa, T., *J. Catal.* **101**, 369 (1986).
20. Grasselli, R. K., Burrington, J. D., and Brazidil, J. F., *Faraday Discuss. Chem. Soc.* **72**, 203 (1982).
21. Brazdil, J. F., Gleaser, L. C., and Grasselli, R. K., *J. Phy. Chem.* **87**, 5485 (1983).
22. Grasselli, R. K., *in* "Handbook of Heterogeneous Catalysis" (G. Ertel, H. Knoezinger, and J. Weitkamp, Eds.), Vol. 5, p. 2302. 1997.